

# QCD Effects in the Decays of TeV Black Holes

Christian Alig<sup>1</sup>, Manuel Drees<sup>1</sup>, and Kin-ya Oda<sup>2</sup>

<sup>1</sup> *Physikalisches Institut, Universität Bonn, Nussallee 12, D53115 Bonn, Germany*

<sup>2</sup> *Theoretical Physics Laboratory, RIKEN, Saitama 351-0198, Japan*

## Abstract

In models with “large” and/or warped extra dimensions, the higher-dimensional Planck scale may be as low as a TeV. In that case black holes with masses of a few TeV are expected to be produced copiously in multi-TeV collisions, in particular at the LHC. These black holes decay through Hawking radiation into typically  $\mathcal{O}(20)$  Standard Model particles. Most of these particles would be strongly interacting. Naively this would lead to a final state containing 10 or so hadronic jets. However, it has been argued that the density of strongly interacting particles would be so large that they thermalize, forming a “chromosphere” rather than well-defined jets. In order to investigate this, we perform a QCD simulation which includes parton-parton scattering in addition to parton showering. We find the effects of parton scattering to remain small for all cases we studied, leading to the conclusion that the decays of black holes with masses within the reach of the LHC will *not* lead to the formation of chromospheres.

# 1 Introduction

The Standard Model (SM) of particle physics is very successful in reproducing experimental data. However, from the theoretical point of view it has several unsatisfactory features. Its perhaps biggest problem stems from the very large hierarchy between the electroweak mass scale  $M_{\text{weak}} \sim 100$  GeV and the (reduced) Planck mass  $M_{\text{P}} \simeq 2.4 \cdot 10^{18}$  GeV. The origin of this hierarchy has no explanation within the SM; worse, it tends to be destroyed by quantum corrections.

In the late 1990's it has been suggested [1, 2] that this problem could be solved by introducing additional spatial dimensions. They could be relatively large if only gravity is allowed to propagate in them, i.e. if all (other) SM fields are bound to a brane with three spatial dimensions. The strength of the gravitational interactions at lengths larger than the radii of these additional dimensions would then be diluted by a factor which is essentially given by the ratio of the volume of these extra dimensions and the appropriate power of the higher-dimensional Planck length. This ratio can be very large even if the higher-dimensional Planck mass  $M_D$  is not far above  $M_{\text{weak}}$ . If this idea is correct, the very large measured value of  $M_{\text{P}}$  is an artefact of using a 3-dimensional description of a world that actually has  $3 + n$  spatial dimensions.

This scenario leads to dramatic predictions for collisions of pointlike particles at high center-of-mass (cms) energy. Collisions at energies around  $M_D$  would likely be dominated by the exchange of gravitons [3], rather than by exchange of SM gauge bosons. Collisions at energies exceeding  $M_D$  could lead to the formation of black holes [4, 5, 6, 7, 8, 9, 10, 11], with cross section being given by the square of the (generalized) Schwarzschild radius. Since this radius actually increases with increasing cms energy, this would lead to “the end of short-distance physics” [5].

These black holes with masses of a few TeV should decay very quickly via the higher-dimension analogue [12] of Hawking radiation [13], into final states on the brane consisting mostly of SM degrees of freedom [14]. Since the Hawking temperature of black holes that can be produced at the LHC is  $\mathcal{O}(100$  GeV), its decay should produce roughly  $\mathcal{O}(20)$  particles with average energy  $\sim 3$  times the Hawking temperature. This decay would appear to be instantaneous to LHC experiments, since the typical lifetime of such a black hole is only  $\mathcal{O}(10^{-27}$  s).

Since these black holes decay into all SM degrees of freedom with approximately equal probability, most final state particles would be strongly interacting quarks or gluons. This leads to the expectation that a typical black hole event at the LHC would contain 10 or so jets plus a few (charged or neutral) leptons and/or photons, each with typical energy of several hundred GeV. This is obviously a very dramatic signature, which should be easy to detect.

However, it has been argued by Anchordoqui and Goldberg [15] that the density of strongly interacting partons just after the decay of the black hole would be so high that they would frequently interact with each other, leading to the formation of a (more or less) thermalized “chromosphere”, i.e. a (nearly) spherical shell of thousands of particles with rather small energies. This final state would also be very easy to detect. However, in this

case the final state would be characterized almost uniquely by the mass of the black hole. More detailed investigations of the primary decay spectrum, which could give information about the number of additional dimensions as well as the spin of the decaying black hole, could then only be performed with the (rather few) primary charged leptons and photons.

It is therefore of some importance to decide whether the assertion of ref.[15] is in fact correct. In this paper we report results of a Monte Carlo simulation of the QCD effects relevant for the decay of TeV black holes, including both parton showering and partonic collisions. This simulation has to keep track of the space–time evolution of the black hole decay products. In contrast, the usual shower codes only keep track of the virtuality of the partons in the shower, but treat the shower itself as instantaneous. This is quite adequate for most applications, since a parton shower only lasts  $10^{-23}$  seconds or so, corresponding to a spatial extension of a few Fermi, many orders of magnitude below the resolution of any conceivable detector. However, if a chromosphere forms at all, it should do so during those  $10^{-23}$  seconds. A careful treatment of the spatio–temporal evolution of the shower is therefore mandatory for us.

We find that the effects of parton–parton scatterings after black hole decay are essentially negligible for a black hole of 5 TeV, and are quite small even for 10 TeV black holes. Even in the latter case, most partons do not scatter. Moreover, most of these (relatively rare) interactions are rather soft, i.e. they do not change the energies, trajectories or virtualities of the participating partons very much. We therefore conclude that the decays of black holes that might be produced at the LHC will *not* lead to the formation of a chromosphere. Black hole event generators that ignore interactions between black hole decay products [16, 17] only make a small mistake.

The remainder of this note is organized as follows. In the next Section we describe the production of TeV black holes, and their subsequent decay through Hawking radiation, in slightly more detail. This determines the initial set–up of the partonic system, which later may or may not develop into a chromosphere. In Sec. 3 we summarize the argument in favor of chromosphere formation, closely following ref.[15]; we also point out some weaknesses in this argument. Sec. 4 is devoted to a description of the simulation program we wrote. In Sec. 5 we present numerical results for the angular correlation between pairs of charged particles, for the overall energy flow of the hadronic black hole decay products, and for the microscopic structure of these events. Finally, Sec. 6 contains a brief summary and outlook.

## 2 Black hole production and decay

Lower bounds on the classical gravitational production cross section of black holes are obtained in [7, 10, 11]. Quantum corrections are estimated in [8, 9]. The implication of the correspondence principle for black holes and strings is considered in [18]. All these results suggest that the black hole production cross section grows geometrically above the

(higher–dimensional) Planck scale:

$$\sigma(\hat{s}) \simeq \pi r_h(M)^2 \propto \hat{s}^{1/(1+n)}. \quad (1)$$

Here,  $n$  is the number of additional spatial dimensions,  $\hat{s}$  is the partonic cms energy, and  $r_h$  is the horizon radius of the  $D = 4 + n$  dimensional Schwarzschild black hole with mass  $M = \sqrt{\hat{s}}$ .\*

$$r_h(M) = \frac{1}{M_D} \left[ \frac{M}{M_D} \frac{2^n \pi^{(n-3)/2} \Gamma\left(\frac{3+n}{2}\right)}{n+2} \right]^{1/(1+n)}. \quad (2)$$

Eq.(1) should hold as long as  $r_h$  is small compared to the size of the additional dimensions, which is true for all cases of interest to LHC experiments.

Astrophysical processes lead to the very strong lower bound  $M_D \gg 10$  TeV for  $n \leq 3$  [19]. For larger  $n$  the lower bound on  $M_D$  comes from searches for the production of gravitons (including their Kaluza–Klein towers) at colliders, yielding  $M_D \geq 0.65$  TeV for  $n = 6$  [20]. It has been argued [21] that the non–observation of black holes produced by very energetic cosmic ray neutrinos yields the slightly stronger bound  $M_D \gtrsim 1$  TeV for  $n \geq 5$ . However, this bound relies on assumptions on the flux of very energetic cosmic neutrinos. We will see shortly that chromosphere formation is most likely for the smallest allowed value of  $M_D$ . To be conservative, we will therefore present numerical results for  $n = 6$  and  $M_D = 0.65$  TeV. In that case according to Eqs.(1), (2) the LHC operating at a proton–proton cms energy of 14 TeV yields cross sections in excess of 200 pb (10 fb) for  $M > 5$  (10) TeV [5]. In other words, the LHC will be a veritable black hole factory if a TeV scale gravity scenario is employed by nature [5, 6].†

We note that the black hole is generically produced with a sizable angular momentum [24]. However, here we only consider the case of vanishing angular momentum. While the spin of the black hole would affect the details of its decay spectrum during the early “spin–down” phase [24, 25, 26], these details are not likely to significantly change the importance of the QCD processes which are the main focus of our analysis.

Once produced, the black hole radiates off its mass  $M$  via Hawking radiation [13] mainly into the brane–localized standard model particles [14].‡ The number spectrum for

\*We use the notation of [15], where  $M_D$  stands for the reduced higher–dimensional Planck mass.

†QCD initial state radiation is, as usual, taken into account by using scale–dependent parton distribution functions, the relevant momentum scale being set by  $1/r_h$  [5]. Numerical simulations indicate [10, 11] that several tens of percent of the cms energy of the colliding partons may escape in form of gravitational radiation. The same calculations show that Eqs.(1), (2) underestimate the cross section for black hole production for fixed  $\hat{s}$ . Nevertheless the energy “lost” in gravitational radiation implies  $M < \sqrt{\hat{s}}$ , in which case the cross section for the production of black holes with a given mass at the LHC might be more than three orders of magnitude smaller than indicated by Eqs.(1), (2) with  $\sqrt{\hat{s}} = M$  [22]. Finally, if a “generalized uncertainty principle” imposes a lower bound on physical lengths of order  $1/M_D$ , the cross section for producing black holes with mass  $M \gg M_D$  at the LHC would also be reduced by several orders of magnitude [23].

‡Possible enhancement effects of bulk graviton emission, especially for highly rotating black holes, have been discussed in [27].

the emission of a spin- $s$  particle with energy  $\omega$  per unit time is

$$\frac{d\dot{N}_s}{d\omega} = \frac{1}{2\pi} \frac{\Gamma_s}{e^{\omega/T} - (-1)^{2s}}. \quad (3)$$

Here the Hawking temperature  $T$  is given by

$$T = \frac{1+n}{4\pi r_h}. \quad (4)$$

The “greybody factor”  $\Gamma_s(E)$  in Eq.(3) is defined to be the absorption rate of the incoming flux with energy  $E$  at spatial infinity:

$$\Gamma_s = \frac{\dot{N}_{\text{in}} - \dot{N}_{\text{out}}}{\dot{N}_{\text{in}}}, \quad (5)$$

when the purely in-going boundary condition is put at the black hole horizon. Physically  $\Gamma_s$  is, in the “time-reversed” sense, the proportion of the radiation that passes through the gravitational potential well from the horizon towards spatial infinity.

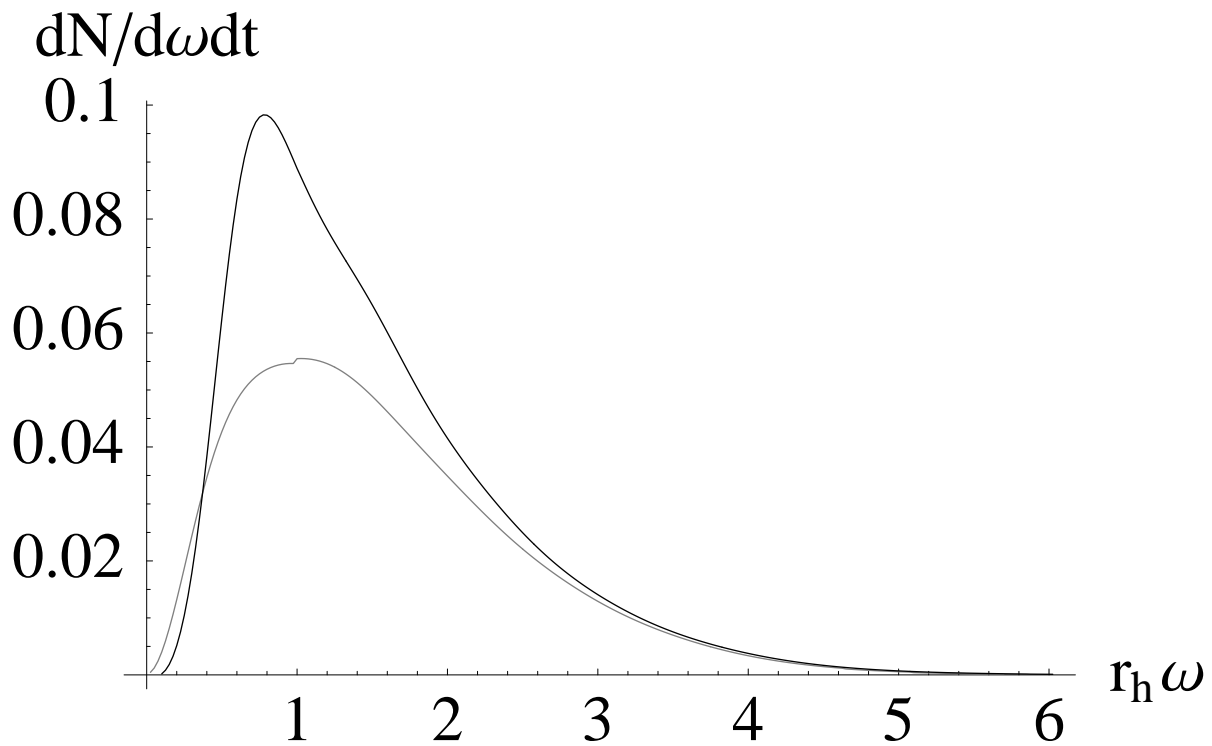


Figure 1: The energy spectrum of gluons (upper, black) and quarks (lower, grey) emitted in black hole decay for  $n = 6$  additional dimensions.  $\omega$  is the energy of the emitted particle, and the Schwarzschild radius  $r_h$  is given by Eq.(2).

Numerical results [26] for the spectra of quarks and gluons produced in the decay of a black hole are shown in Fig. 1. In principle Eqs.(3) and (4) predict that the spectrum of black hole decay products changes with time: as more energy is radiated off, the mass of the black hole becomes smaller. Eq.(2) shows that this also reduces its radius, which according to Eq.(4) increases its temperature.\* For simplicity we employ the “sudden decay approximation” [6] where the entire decay spectrum is calculated using a fixed black hole mass.

All degrees of freedom with a given spin are emitted with equal probability in black hole decay; however, Fig. 1 shows that the greybody factors do depend on the spin. In order to include this effect, we define the integrals over the decay spectra

$$I_s = \int_0^\infty \frac{d\dot{N}_s}{d\omega} dz, \quad (6)$$

where  $z = \omega r_h$  is the dimensionless variable shown in Fig. 1. Numerically,  $I_{1/2} \simeq 0.115$ ,  $I_1 = 0.155$ . In our simulation we are primarily interested in the question whether quarks and gluons produced in black hole decay will thermalize. Since scattering cross sections for heavy quarks are smaller than those for massless quarks, we conservatively assume that only  $u, d, s, c$  quarks and gluons are emitted in black hole decays. The relative abundance of gluons is then on average given by

$$\frac{\langle N_g \rangle}{\langle N_g \rangle + \langle N_q \rangle} = \frac{8I_1}{8I_1 + 24I_{1/2}}. \quad (7)$$

An analogous argument shows that about 75% of the black hole mass will be radiated into quarks and gluons.†

The total (average) number of particles produced in the decay of a single black hole can be estimated from the integrals

$$\tilde{I}_s = \int_0^\infty z \frac{d\dot{N}_s}{d\omega} dz; \quad (8)$$

numerically,  $\tilde{I}_{1/2} = 0.181$ ,  $\tilde{I}_1 = 0.231$ . The average energies (in units of  $r_h^{-1}$ ) of the produced particles are given by the ratios  $\tilde{I}_s/I_s$ . Numerically, the average energy of a quark or gluon

---

\*Since Fig. 1 effectively shows the spectrum in units of the inverse black hole radius, it includes all the information required for including this effect in the simulation. However, these semi-classical results only hold for  $M \gg \omega$ ; they may therefore not describe the late stages of black hole decay adequately. In fact, it has been argued [28] that a black hole will not evaporate completely, but leave behind a stable or at least long-lived, and possibly charged, remnant with mass  $\sim M_D$ . We do not consider this possibility in our work.

†Massive gauge and Higgs bosons produced in black hole decay frequently also decay into quarks. However, these bosons have much longer lifetimes than the black hole itself. The quarks produced in their decays therefore come too late to contribute to the formation of a chromosphere, although they might get trapped in the chromosphere [15] should it indeed form.

is  $\langle E_q \rangle = 313$  (283) GeV and  $\langle E_g \rangle = 296$  (268) GeV for  $M = 5$  (10) TeV. Using the fact that about 75% of the total energy goes into hadrons, this gives average parton multiplicities

$$\begin{aligned}\langle N_q \rangle &= 8.4 \quad (18.6) \\ \langle N_g \rangle &= 3.8 \quad (8.3),\end{aligned}\tag{9}$$

for  $M = 5$  (10) TeV, where  $N_q$  counts both quarks and antiquarks. Choosing a larger higher-dimensional Planck scale  $M_D$  would lead to higher Hawking temperature  $T$ , and hence to fewer, more energetic, primary black hole decay products; this would obviously reduce the probability of parton-parton scattering.

Finally, Eq.(3) also allows to compute the lifetime of the black hole. To that end, one computes the time derivative of the mass of the black hole,

$$\frac{dM}{dt} = \int_0^\infty \omega \frac{d\dot{N}}{d\omega} d\omega.\tag{10}$$

If we set  $t = 0$  for the time of black hole production, its lifetime  $\tau_{\text{bh}}$  is defined by  $M(\tau_{\text{bh}}) = 0$ . Eq.(3) shows that the rhs of Eq.(10) is  $\propto r_h^{-2}$ . The use of Eq.(2) then leads to [5]

$$\tau_{\text{bh}} = \Gamma_{\text{bh}}^{-1} = \frac{C}{M_D} \left( \frac{M}{M_D} \right)^{(n+3)/(n+1)}.\tag{11}$$

The coefficient  $C$  can be computed by numerically integrating the spectra shown in Fig. 1, leading to  $C \simeq 0.2$ . Eq.(11) then gives  $\Gamma_{\text{bh}} = 240$  (100) GeV for  $M = 5$  (10) TeV and  $M_D = 0.65$  TeV, corresponding to lifetimes of order  $10^{-27}$  seconds.

Having presented the relevant properties of the partonic final state that emerges from black hole decay, we are now ready to discuss whether interactions between these partons might lead to formation of a chromosphere.

### 3 Arguments for and against chromosphere formation

The argument by Anchordoqui and Goldberg [15] starts from the observation that the parton number density  $n$  after black hole decay is quite high: roughly  $\mathcal{O}(10)$  partons are distributed over a sphere with radius  $\sim c\tau_{\text{bh}}$ . They estimate the rate  $\Gamma$  of bremsstrahlung reactions (which increase the total number of partons) as  $\Gamma = n c \sigma_b$ , with

$$\sigma_b \simeq \frac{8\alpha_s^3}{\Lambda^2} \ln \left( \frac{2Q}{\Lambda} \right),\tag{12}$$

where  $\alpha_s$  is the strong coupling constant and  $Q$  the initial energy of the parton in the rest frame of the black hole; the energy scale  $\Lambda$  is estimated as the inverse of the radius of the expanding shell of partons. This leads to a total interaction rate per parton [15]

$$\mathcal{N}_{\text{int}} \simeq 0.15 \frac{N_{q,\text{init}}}{10} \left( \frac{\alpha_s(Q_{\text{min}})}{0.2} \right)^3 \ln \left( \frac{2Q}{Q_{\text{min}}} \right) \ln \left( \frac{\Gamma_{\text{bh}}}{Q_{\text{min}}} \right).\tag{13}$$

For  $Q \simeq 400$  GeV and initial parton number  $N_{q,\text{init}} = 10$  Eq.(13) predicts about 3 interactions per parton even with minimal momentum transfer  $Q_{\text{min}} = 9$  GeV; this increases to  $\sim 30$  interactions for  $Q_{\text{min}} = 1.8$  GeV (the mass of the  $\tau$  lepton). Anchordoqui and Goldberg argue that partons that interact so frequently must thermalize, leading to the formation of an expanding shell of particles with approximately thermal energy distribution.<sup>‡</sup>

This argument has several weaknesses. To begin with, most QCD interactions are rather soft, as seen by the factor  $1/\Lambda^2$  in Eq.(12). Similarly, most emitted gluons will be soft and/or collinear; this leads to the logarithmic factor in the cross section (12). In other words, a “typical” interaction may not change the energies and momenta of the participating partons very much, and may only lead to the emission of a soft and/or collinear gluon. Such interactions would *not* impede the formation of well-defined hadronic jets. In fact, during a QCD parton cascade, many gluons will in any case be emitted from the partons produced in a given “hard” process; most of these gluons will also be soft and/or collinear. This gives rise to finite widths and masses of hadronic jets, but does not destroy them.

Secondly, Anchordoqui and Goldberg seem to have overlooked the fact that a scattering reaction takes a finite time: according to the uncertainty principle, the time at which a reaction with energy exchange of  $\mathcal{O}(\Lambda)$  occurs can only be determined with an intrinsic uncertainty of order  $\mathcal{O}(1/\Lambda)$ . Most reactions have  $\Lambda \sim r^{-1}$  [15],  $r$  being the radius of the expanding shell of particles. Loosely speaking, a particle “has time” for only one such reaction while traveling a distance  $\mathcal{O}(r)$ .

The formation of a chromosphere seems unlikely on purely phenomenological grounds. Note that the number of interactions per parton is proportional to the number of initial partons. If ten initial partons lead to a chromosphere, five or six initial partons should at least show significant effects from these interactions. The observation of events with six well-defined jets has been reported by both the UA2 [29] and CDF [30] collaborations. CDF finds fair agreement between observations and QCD parton shower simulations (based on leading-order matrix elements). They demand that the total invariant mass of the 6-jet system exceed 520 GeV, while each jet should have a transverse momentum of at least 20 GeV. Using  $N_{\text{init}} = 6$ ,  $Q = 30$  GeV and  $\Gamma_{\text{bh}} \rightarrow M_{6\text{-jet}} = 500$  GeV setting the scale for the initial hard reaction, Eq.(13) predicts  $\mathcal{N} \simeq 0.7$  (9.5) interactions per parton for  $Q_{\text{min}} = 9$  (2) GeV. We find it difficult to believe that such high interaction rates would leave no imprint in the properties of the observed events, given that 3 (30) interactions are supposed to lead to nearly complete thermalization.

Even if a nearly thermal chromosphere does not form, parton-parton scattering might still have significant impact on the hadronic final state from black hole decay. Given the complexity of QCD processes even in the absence of parton-parton scattering, a quantitative investigation of their effect can only be performed with the help of a QCD simulation

---

<sup>‡</sup>In contrast, the authors of ref.[5] state that the shell of black hole decay products is too thin to thermalize; however, no quantitative estimate of the effects of interactions between these decay products is given there.



program. This is the topic of the next Section.

## 4 Simulation

We saw in the previous Section that a quantitative analysis of the effects of parton–parton scattering is only possible if we also treat the QCD parton showers that occur whenever a large four–momentum is transmitted to strongly interacting particles. This implies that we need to follow the spatio–temporal development of these QCD showers. In this Section we first outline the general philosophy of our approach; a more detailed description of the various stages treated by our code will be given in the subsequent Subsections.

Numerical codes that simulate parton showers are probabilistic, i.e. they operate with squared amplitudes. Quantum mechanical interference effects can therefore only be treated approximately (e.g. through angular ordering [31], whereby subsequent gluons are emitted at smaller and smaller angles.) The basic idea is that partons emerging from a hard reaction (scattering or decay) initially have time–like virtuality, which is reduced by “branching off” additional partons. This can be justified by the observation that in a complete calculation of the relevant Feynman diagrams, final state partons emitting additional partons indeed have to have time–like virtualities. The beauty of such showering algorithms is that they exploit QCD factorization theorems to sum such higher order processes to all orders in perturbation theory, albeit (usually) only with leading logarithmic accuracy.

Most of these codes follow the “evolution” of this shower not in time, but in an energy variable, which in the simplest case is given by the virtuality of the partons in the shower; since we are dealing with final–state showers, the partons in question have time–like momenta, i.e. the shower has the same kinematics as a cascade of two–body decays. (In this analogy, the lifetime of the decaying particles would be given by the inverse virtuality of the particles in the shower.)

According to quantum mechanics, one cannot simultaneously determine this shower energy scale and the (proper) time of a branching. Unfortunately for our application we need to do precisely that. A certain additional abuse of the principles of quantum mechanics is therefore inevitable. We do this by identifying the *uncertainty* in time, as determined by the uncertainty principle, with the actual *duration* of a given process. We use this identification both for the branching and for parton–parton scattering; in the former case, the time is given by the inverse of the virtuality of the branching parton, whereas the time needed for a scattering is given by the (space–like) virtuality of the parton exchanged in this scattering reaction. Note that neither two branching steps, nor two scatterings, involving the same partons can occur at the same time. In the absence of scattering, the evolution in time would therefore strictly match the evolution towards smaller virtualities. Moreover, between branching or scattering events, the partons are taken to propagate along their classical paths. Note that this evolution is nonetheless probabilistic, since after each branching or scattering the 4–momenta of the outgoing partons are chosen randomly, with distributions determined by perturbative QCD (and subject to energy–momentum conservation).

We only aim at leading logarithmic accuracy. This means that we only use leading order cross sections, and only include  $2 \rightarrow 2$  scattering processes; later gluon emission, which is treated explicitly in the estimates of interaction rates in ref.[15], is taken into account by the subsequent shower evolution. In fact, including  $2 \rightarrow 3$  processes in the scattering reactions would lead to double counting. Scattering reactions can nevertheless increase the particle multiplicities, since they can *increase* the virtuality of the participating particles; in contrast, each branching reduces this virtuality. Moreover, the scattering can change the 3-momenta of the particles, thereby potentially destroying the jet structure. As mentioned in the previous Section, one needs large scattering angles in order to establish a chromosphere from an initially small number of very energetic partons.

As usual, we treat showering and hard scattering independently, i.e. we apply QCD factorization. This requires that the scattering indeed be sufficiently hard; that is, the absolute value of the four-momentum exchanged in the scattering reaction must be (much) larger than the virtualities of the partons in both the initial and final state. However, as already noted, the partons in the final state may be more off-shell than those in the initial state. Note also that we should not include initial state showering in our approach, since each “initial state” of a scattering reaction is part of the extended final state shower that follows the Hawking evaporation of the black hole; including initial state radiation would therefore also lead to double counting.

Our simulation starts with a rather small number of energetic, and far off-shell, partons, using the results of Section 2. It then uses small time steps to follow the parton shower and/or scattering of all partons. This phase ends when all partons are (nearly) on-shell and far apart from each other, so that neither further branching nor further scattering is possible. When the particles virtualities reach the QCD scale  $\Lambda_{QCD}$ , hadronization will take place and the data of the final particles will be stored for statistical analysis.

The simulation code has been written nearly from scratch in C++, although the global structure is based on the VNI 4.12b Monte Carlo simulation [32, 33] using its particle record and a selection of modified routines from it. The VNI particle record uses the “Les Houches” format, extended to hold information necessary for the full space-time evolution of the partons. VNI 4.12b was originally written in order to simulate ultra-relativistic heavy-ion collisions; in that case, multiple partonic scattering reactions are certainly important, and had to be modeled carefully, making this code a good starting point for our work. In contrast, scattering in the final state is thought to be unimportant for hard reactions involving  $e^\pm$  and/or  $p/\bar{p}$  in the initial state.

We also use some routines from the PYTHIA Monte Carlo simulation [34]. For numerical integration and a simulation grade random number generator the GNU Scientific Library [35] for C/C++ was used.

## 4.1 Initial setup

As in ref.[15] we randomly distribute the initial partons inside a shell with thickness equal to the black hole lifetime  $\tau_{bh}$  (11) around the decayed black hole with radius (2). Quarks and gluons are generated separately, with average multiplicities given by Eq.(9) and energy

distributions according to Fig. 1. The momenta of most partons are chosen randomly inside that half of the solid angle which points away from the black hole, as seen from the location at which the particle is created. Choosing the partons to be always emitted radially by the black hole, which would be proper for non-rotating black hole, would make future collisions between them impossible in the absence of showering; our choice therefore increases the possibility of parton-parton scattering.\* The 3-momentum of the last parton is taken such that the total 3-momentum in the black hole rest frame is zero.† This is not absolutely necessary, because the 3-momenta of the strongly interacting particles alone do not have to add up to zero, but it allows a good control of the simulation.

Next, quark flavors are assigned randomly. We do not include the top and bottom quark because we cannot assume them to be massless in all possible collisions when we are using the massless QCD scattering amplitudes; indeed, top production is likely to be somewhat suppressed since for our choice of parameters, the Hawking temperature is somewhat below  $m_t$ . Charge conservation is not enforced in our initial setup taking into account that the black hole also radiates off other particles like leptons. However we take care that the charges add up to some integer.

We set the maximal initial virtualities of the partons equal to their energies; the actual values of these virtualities will be chosen by the shower algorithm described in a subsequent Subsection. This choice of maximal virtuality reproduces features of hadronic  $Z$  decays fairly accurately, when starting from leading order,  $Z \rightarrow q\bar{q}$ , decays.‡

After the initial setup the program enters the main loop, which simulates the space-time evolution of the parton cascade. This evolution is determined by two processes, parton scattering and branching, which are described in the next two Subsections.

## 4.2 Parton scattering

Every possible pair of partons is boosted from the black hole rest frame into its cms frame, and it is checked if it has reached its closest possible distance. In the next step it is checked whether partons which reached their closest distance undergo a collision. We are using the cascade approach [36] for this purpose, according to which a collision takes place if the closest distance of the parton pair is within the radius defined by the total cross section of

---

\*Non-radial emission should occur during the spin-down phase, with quite complicated angular dependence [24, 25, 26]. Since most of the energy is released after the black hole has shed its spin, our treatment most likely over-estimates the probability of parton-parton scattering.

†This is not always possible, given that the energy of this parton has already been fixed and its virtuality must be smaller than this energy. If no solution is found, the event is abandoned, and the routine for generating the initial set-up makes a new attempt.

‡One might argue that this choice is not appropriate for black hole decay, since black holes are not pointlike, unlike  $Z$  bosons. However, for choices of  $M_D$  and  $M$  relevant for LHC phenomenology, the scales  $1/r_h$  or  $\Gamma_{bh}$  that describe the spatio-temporal extension of the black hole are quite close to the average energies of the decay partons; note also that the final results will only depend logarithmically on the maximal initial virtuality.

the specific process,

$$|\mathbf{r}_a - \mathbf{r}_b|_{\min} \leq \sqrt{\frac{\hat{\sigma}_{ab}}{\pi}}. \quad (14)$$

If there is more than one possible scattering channel for two partons the total cross section will be the sum of the cross sections for all possible final states,

$$\hat{\sigma}_{ab} = \sum_{c,d} \hat{\sigma}_{ab \rightarrow cd}. \quad (15)$$

The individual cross sections are calculated numerically by integrating the corresponding differential cross sections

$$\hat{\sigma}_{ab \rightarrow cd} = \int_{\hat{t}_{\min}}^{\hat{t}_{\max}} \left( \frac{d\hat{\sigma}(\hat{s}, \hat{t}, \hat{u})}{d\hat{t}} \right)_{ab \rightarrow cd} d\hat{t}, \quad (16)$$

with Mandelstam variables  $\hat{s} = (p_a + p_b)^2$ ,  $\hat{t} = (p_a - p_c)^2$ ,  $\hat{u} = (p_a - p_d)^2$ . The choice of the upper and lower bounds  $\hat{t}_{\max}$ ,  $\hat{t}_{\min}$  in equation (16) requires some care. When two on-shell partons are scattering, the matrix elements for the  $(2 \rightarrow 2)$  QCD cross sections diverge for forward ( $\hat{t} \rightarrow 0$ ) and/or backward ( $\hat{u} \rightarrow 0$ ) scattering, thus a minimal momentum transfer is needed that determines  $\hat{t}_{\max}$  and  $\hat{t}_{\min}$  for given  $\hat{s}$ . In this case we take the commonly used value (in the parton-parton cms) of  $p_{\perp \min} = 1$  GeV; this requires  $\sqrt{\hat{s}} > 2$  GeV. Collisions with  $p_{\perp} < 1$  GeV are considered to be soft and are not evaluated since only collisions generating high transverse momentum can change the jet structure of the event.

Collisions with at least one virtual particle in the initial state need special treatment, since off-shell initial or final partons lead to non gauge invariant  $(2 \rightarrow 2)$  amplitudes [36]. The authors of [36] solve this problem by combining the scattering with space- or time-like branching in a single (rather large) time step so that at the end of a scattering only on-shell particles are left and only on-shell particles will scatter again. This should be sufficient for the simulation of heavy ion collisions, where (nearly) all virtualities and exchanged 4-momenta are quite small. However, in our case this procedure would allow a parton to instantaneously\* shower off a virtuality of hundreds of GeV and then undergo a collision with momentum exchange of only a few GeV. This does not make sense, since such a relatively soft collision would take much more time than the (initial part of) the showering; moreover, the (many) particles produced in the shower might undergo scatterings of their own.

We therefore take another approach: we allow virtual particles to take part in a collision only if the scattering scale  $Q_{\text{scatt}}^2$  is at least as high as half the sum of the virtualities  $Q_a^2$ ,  $Q_b^2$  of the particles  $a$  and  $b$  in the initial state,

$$Q_{\text{scatt}}^2 \geq \frac{Q_a^2 + Q_b^2}{2}. \quad (17)$$

---

\*Our program uses much shorter time steps than the original VNI code, typically  $\sim 2 \cdot 10^{-4}$  GeV $^{-1}$  initially. We checked that choosing even shorter steps does not change the result.

In this case the scattering will at least not take longer than the parton shower up to that point. Moreover, it can be hoped that the scattering is hard enough that the virtuality of the particles in the initial state becomes irrelevant, so that we can describe the scattering using massless ( $2 \rightarrow 2$ ) QCD cross sections. In fact, basically the same condition is chosen by the usual QCD simulators when setting the showering scale for initial state radiation, although in these programs the scattering scale  $Q_{\text{scatt}}^2$  is fixed first. In our simulation the scattering scale is taken to be

$$Q_{\text{scatt}}^2 = \frac{\hat{t}\hat{u}}{\hat{s}} \simeq \mathbf{p}_{\perp}^2. \quad (18)$$

This also fixes the scale in the running strong coupling constant,

$$\alpha_s(Q_{\text{scatt}}^2) = \frac{12\pi}{25 \log\left(\frac{Q_{\text{scatt}}^2}{\Lambda_{QCD}^2}\right)}, \quad (19)$$

where we took  $N_F = 4$  active flavors and QCD scale  $\Lambda_{QCD} = 0.2$  GeV. The requirement (17) determines the boundaries of the integration over  $\hat{t}$  in (16):

$$\hat{t}_{\text{min,max}} = \frac{1}{2} \left( -\hat{s} \mp \sqrt{\hat{s}^2 - 4Q_{ab}^2\hat{s}} \right), \quad (20)$$

where  $Q_{ab}^2 = \frac{Q_a^2 + Q_b^2}{2}$ .

We did not include ( $2 \rightarrow 1$ ) fusion processes like  $g + g \rightarrow g^*$  (with  $g^*$  being off-shell), since the first branching of the produced off-shell parton would again result in a  $2 \rightarrow 2$  process, leading to double counting. It could be argued that we should also require  $Q_{\text{scatt}} \geq 1/|\mathbf{r}_a - \mathbf{r}_b|_{\text{min}}$ . However, this would exclude interactions between partons that happen somewhat before or after the time of their closest approach, which seems unphysical. We therefore do not impose this additional requirement, which would reduce the number of partonic scatterings significantly. In fact, the opposite requirement,  $Q_{\text{scatt}} < 1/|\mathbf{r}_a - \mathbf{r}_b|_{\text{min}}$ , seems more reasonable, since according to the uncertainty principle a highly virtual exchanged parton can only travel a very short distance. We do not impose this constraint, i.e. we allow very large momentum exchange also between relatively distant partons. This again increases the importance of collisions, since a large  $Q_{\text{scatt}}$  is required for a collision to modify the jet structure. However, we will see that not imposing this upper bound on  $Q_{\text{scatt}}$  has very little effect in practice, since high values of  $Q_{\text{scatt}}$  are in any case very unlikely.

In some rare cases one parton has two possible collision partners in a single time step. In that case for both partners cross section and distance will be checked. If only one collision takes place this will be the one evaluated. If both collisions would take place only the one with the larger cross section will be evaluated.

After a pair of particles has been identified as colliding, the scattering kinematics can be generated. For initial states which have more than one channel, the final state is chosen according to the probability given by the relevant total cross sections. Next the value of  $\hat{t} \in [\hat{t}_{\text{min}}, \hat{t}_{\text{max}}]$  is generated, with distribution given by the corresponding differential cross

section  $d\hat{\sigma}/d\hat{t}$  (normalized to unity). The initial particle pair is boosted into its cms frame and put on-shell. The absolute value of the transverse momentum of the final particles is given by  $Q_{\text{scatt}}^2$  as determined by the chosen value of  $\hat{t}$ . The azimuthal scattering angle, which fixes the direction of the  $\mathbf{p}_\perp$  vectors, is chosen randomly, with flat distribution between 0 and  $2\pi$ .

Finally the virtualities of the outgoing particles are created by the branching routine (see the next Subsection) and color charges are assigned according to the color flow of the specific process. It should be noted that in case of the scattering of virtual particles, the virtuality after scattering can become even lower than before, since  $Q_{\text{scatt}}$  is the *maximal* virtuality of the particles in the final state. We see no physical reason why such virtuality-reducing scattering reactions should be suppressed.

Due to the lifetime of a virtual (exchanged) particle the scattering will take a finite amount of time determined by the scattering scale. In the rest frame of the black hole this time is given by

$$\tau_{\text{scatt}} = \frac{\gamma_{ab}}{Q_{\text{scatt}}}, \quad (21)$$

where  $\gamma_{ab} = (E_a + E_b)/\sqrt{\hat{s}_{ab}}$  is the boost factor between the cms of colliding partons  $a$  and  $b$  and the black hole rest frame. During this time the colliding particles are not allowed to collide again, nor can they branch off additional partons; in fact, in quantum mechanics one cannot say whether the parent partons  $a, b$  or the children  $c, d$  exist during the period  $\tau_{\text{scatt}}$ . After the scattering time is over the partons are able to initiate final state radiation or collide again.<sup>†</sup>

### 4.3 Parton branching

While the inclusion of partonic collisions is the main new ingredient of our simulation, we will see that parton branching plays a far more important role in determining the characteristics of the final state. We model this using a modified version of the relevant routine of VNI 4.12b, which in turn is based on the PYTHIA branching algorithm [34, 37, 38].

The modifications implemented by us address the need to do branching for a single parton, instead of treating two partons at once as is done normally in order to ensure 4-momentum conservation. To make sure we can conserve energy and momentum for a single parton we always have to determine the virtualities at which the parton branches one step ahead in the branching algorithm: the kinematics of  $a \rightarrow b + c$  can only be fixed if the “masses”, i.e. (time-like) virtualities, of all three participating partons are known. Our version of the routine therefore determines the virtualities of  $b$  and  $c$  earlier than the

---

<sup>†</sup>In principle it might be more appropriate to place this “dead time” symmetrically around the time of closest approach, rather than letting it start at the time of closest approach. However, this would be technically difficult, since the program would then have to go back in time, and “un-do” any possible branchings that happened in the “dead” period before the time of closest approach. Since by construction  $Q_{\text{scatt}}$  is larger than the virtuality of the scattering particles, this asymmetric placement of the “dead time” should not matter much in practice.

original routine does. Note that these actual virtualities are typically much smaller than the corresponding maximal values; this is the reason why energetic partons, with initial *maximal* virtualities given by their energies, typically produce quite narrow jets. Another modification is the introduction of the scattering-induced “dead time” described at the end of the previous Subsection, during which partons are not allowed to branch.

Just like scattering reactions, the branching  $a \rightarrow b + c$  also takes a finite amount of time in our simulation, given by

$$\tau_{\text{branch}} = \frac{\gamma_a}{Q_a} = \frac{E_a}{Q_a^2}, \quad (22)$$

with  $\gamma_a = E_a/Q_a$  describing the boost from the rest frame of parton  $a$  to that of the black hole. In our simulation this is treated like the lifetime of a decaying particle, i.e. the probability of an “active” parton  $a$  to branch during the time step  $dt$  is given by [32, 33]

$$P_{\text{branch}} = 1 - e^{-dt/\tau_{\text{branch}}} \simeq \frac{dt}{\tau_{\text{branch}}}, \quad (23)$$

where the second, approximate equality holds for the (realistic) situation  $dt \ll \tau_{\text{branch}}$ . Note that each parton is checked for possible scattering before it is checked for branching. In our treatment partons  $b, c$  are created instantaneously if a branching occurs, i.e. they are allowed to undergo scattering immediately.\* This can be justified from the requirement (17), which ensures that scattering reactions are much faster than branchings. Imposing a branching “dead time” of (some fraction of)  $\tau_{\text{branch}}$  on  $b, c$  before they are allowed to scatter would obviously reduce the number of parton–parton scatterings, although numerically this effect is not very large. The 4–momenta of partons  $b, c$  are chosen as in the PYTHIA branching algorithm [34].

There are three situations in which the branching routine is used. First, all initial partons which have some maximum virtuality from black hole decay are sent through the branching routine once, in order to determine their actual starting virtuality for the simulation. Secondly, the normal use when every time step all partons which have any time–like virtuality left, and which did not scatter recently, are sent through the routine to undergo branching with probability given by Eq.(23). Third, similar to the first case, the two partons coming out of a hard scattering which took place at the scale  $Q_{\text{scatt}}^2$  are sent through the branching routine to determine the actual virtualities they will start to propagate with.

The next step after the parton branching algorithm is to propagate all partons freely by one time step. Then the simulation calculates the average distance between all pairs of partons to see if it exceeds the QCD scale  $1/\Lambda_{\text{QCD}}$ , at which point the partonic simulation loop can be aborted. If the abort condition is met hadronization will take over, or else time is increased by one time step and the simulation loop starts again. For details of the hadronization algorithm we again refer to the documentation of PYTHIA [34].

---

\*These partons are created at slightly different locations, as determined by the uncertainty principle; moreover, they are moving away from each other. These two partons can therefore not scatter on each other, even if they are very close, but they can scatter on other partons.

## 5 Results

We are now ready to present some numerical results. As stated in Sec. 2, we set the higher-dimensional Planck scale to its lower bound,  $M_D = 0.65$  TeV, since this maximizes the number of initial partons, and hence the number of parton-parton interactions within a given black hole decay. We also consider relatively heavy black holes, with  $M = 5$  and 10 TeV. Recall that decays of heavier black holes are characterized by lower temperatures, and hence higher multiplicities; however, the production cross section for black holes with mass exceeding 10 TeV is certainly negligible at the LHC.

Since the initial set-up is created totally randomly there are large event-to-event fluctuations of the number and energies of the initial partons. One therefore needs sufficient statistics to make reliable statements about average quantities; the results presented below are based on 200 events for each run. In order to illustrate the effects of parton-parton interactions, we made separate runs for each black hole mass where these interactions were turned on or turned off. In the latter case the spatio-temporal evolution of the parton shower is irrelevant, i.e. our program reproduces standard (PYTHIA) showering for the given set-up of original partons.

If black hole decays led to formation of a chromosphere, observables based on jets would no longer be useful. In the following Subsections we therefore analyze the distribution of two observables whose definition does not assume the existence of jets: angular correlations between energetic charged hadrons, and the overall energy flow. Of course, the observables are chosen such that their distribution would be greatly affected if parton-parton scattering did indeed lead to formation of a chromosphere. In the last Subsection we will interpret these results with the help of the time structure of the parton shower that develops after typical black hole decays.

### 5.1 Angular correlation

After hadronization we are left with a large number of charged, long-lived particles (mostly charged pions and kaons and some protons) as well as photons and neutral hadrons. In this first analysis we focus on charged particles because their momenta can be measured accurately using tracking information. We only consider particles with an energy (in the black hole rest frame) above 4 GeV; the number of charged particles passing this cut is denoted by  $N_{\text{ch}}$ . This cut should largely remove particles from the underlying event which have nothing to do with black hole decay, and which have not been included in our simulation.

We compute the angles  $\theta$  between any two of these charged particles; altogether there are  $N_{\text{pair}} = N_{\text{ch}}(N_{\text{ch}} - 1)/2$  such pairs. The resulting distribution is binned in  $\cos \theta$ . Because  $N_{\text{ch}}$  can vary a lot from event to event, we normalize the distribution for each event to  $N_{\text{pair}}$ , before averaging over the 200 generated events.

Let us first consider some simple situations, in order to get a feeling for what kind of distribution to expect. The simplest case, which certainly does not describe black hole decay, would be events with two back-to-back jets, each of which contains the same number



$N_{\text{ch}}/2$  of charged particles. In this case  $N_{\text{ch}}^2/4 - N_{\text{ch}}/2$  pairs would have an angle near zero between the particles of the pair because they reside inside the same jet; the remaining  $N_{\text{ch}}^2/4$  pairs would have an angle near  $\pi$  between the particles of the pair because the particles are in different jets. In the limit of large  $N_{\text{ch}}$  these numbers will become almost equal, leading to peaks at 1 and  $-1$  in our plot which have approximately the same height.

A case that is closer to what one may expect from the decay of a black hole would be an event with  $n_j$  jets. Let us keep the assumption that each of these jets contains exactly the same number  $N_{\text{ch}}/n_j$  of energetic charged particles. In this case there are

$$\frac{N_{\text{ch}}}{2} \left( \frac{N_{\text{ch}}}{n_j} - 1 \right) \quad (24)$$

pairs residing in the same jet; the remaining  $N_{\text{ch}}^2(n_j - 1)/(2n_j)$  pairs of charged particles are in different jets. We thus see that the fraction of all pairs that reside inside the same jet will decrease when the number of jets increases, i.e. the peak in our distribution at  $\cos\theta = +1$  will become smaller. Moreover, for  $n_j \gg 2$  randomly distributed jets the peak at  $\cos\theta = -1$  will vanish because momentum conservation no longer requires any two jets in the event to be back-to-back. After averaging over many events all the angles between different jets contribute more or less equally. In this case we therefore expect a smooth distribution (although momentum conservation may still lead to a slight increase of the correlation function at negative  $\cos\theta$ ) with only one peak at  $\cos\theta = +1$ . The distribution should remain qualitatively the same in the more realistic scenario where we allow different jets to contain different numbers of charged particles, although eq.(24) will then no longer be valid.

On the other hand, if we assume that a chromosphere is indeed spherical, the correlation function should become almost perfectly flat; in particular, we would not expect any visible peak at  $\cos\theta = +1$ .

Figs. 2 show results for black hole mass  $M = 5$  TeV (top) and 10 TeV (bottom), with (red) and without (black) parton-parton scattering. Clearly for both black hole masses there is still a strong peak at  $\cos\theta = 1$ , leading to the conclusion that we should expect a jet structure after black hole decay. The peak becomes smaller for a heavier black hole; this is expected from the qualitative discussion presented above, given the increasing initial parton multiplicity, see Eq.(9). The rise of the distribution towards  $\cos\theta = -1$  is also more pronounced for smaller black hole masses, again as expected from our qualitative discussion. For  $M = 5$  TeV, parton-parton scattering has essentially no effect on this distribution. For  $M = 10$  TeV, it leads to a very slight broadening of the peak at  $\cos\theta = +1$ ; however, given the uncertainties of our simulation, we do not claim that this effect is significant.

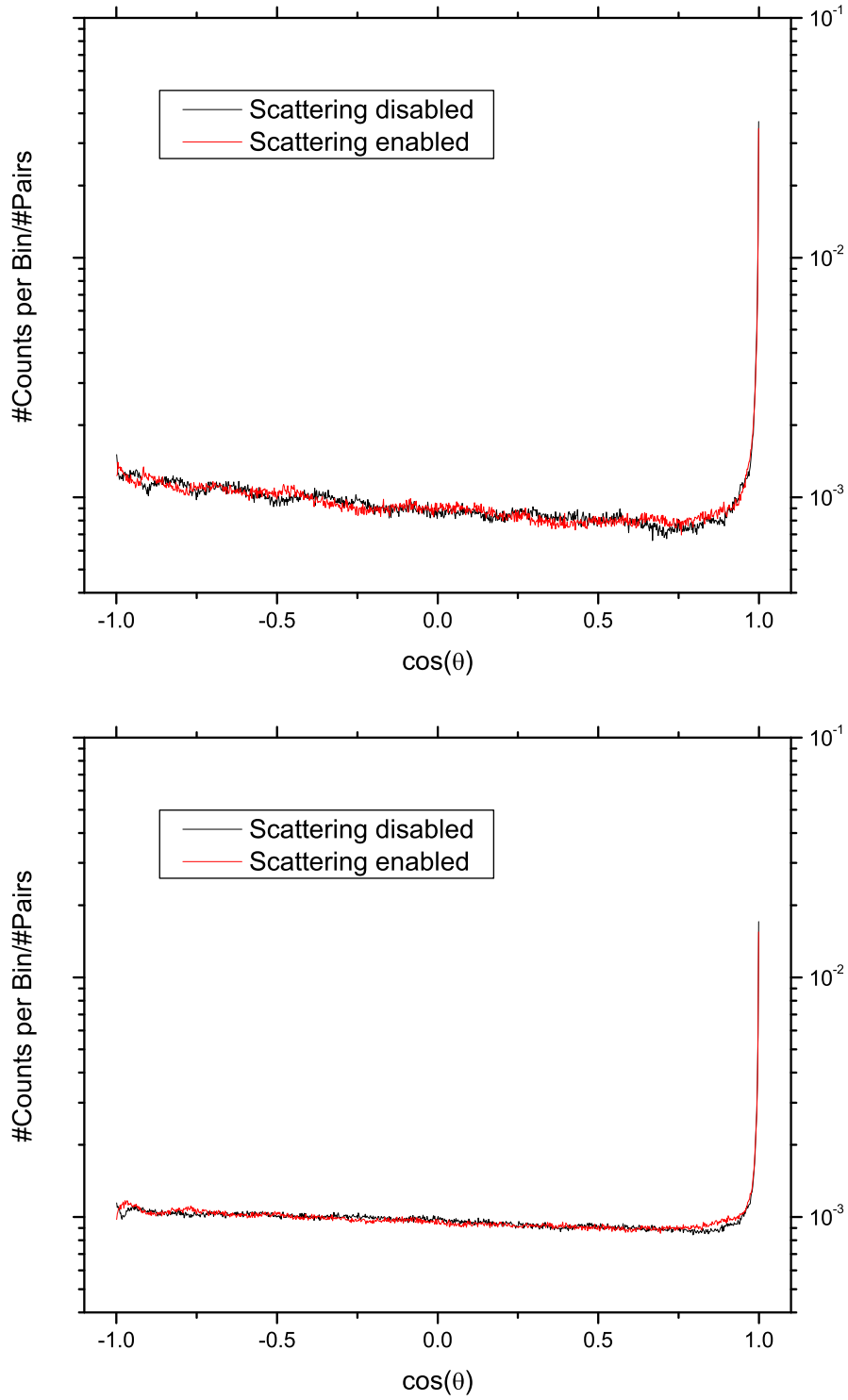


Figure 2: The angular correlation function for charged particles from black hole decay with  $E > 4$  GeV, for black hole mass  $M = 5$  (top) and 10 TeV (bottom), obtained by binning into 1,000 bins. The red and black curves have been obtained including and omitting parton-parton scattering, respectively.

## 5.2 Total energy flow

The second quantity we investigate is the total energy flow from the hadronic black hole decay products. Here we envision a calorimetric measurement. We therefore divide phase space into azimuthal angle  $\phi \in [0, 2\pi]$  and pseudo-rapidity  $\eta \in [-4, 4]$ , with 15 bins in  $\phi$  and 30 bins in  $\eta$ . For each of these 450 “calorimeter cells” the total visible energy is calculated, including hadrons and photons from hadronic decay, but no neutrinos or muons. We present the result by plotting the number of cells with deposited energy  $E_{\text{cell}} \leq E_{\text{max}}$  as function of  $E_{\text{max}}$ .

Let us again first discuss the possible shapes of this distribution for different final parton configurations. If a chromosphere forms, we expect a very large number of hadrons in the final state, each of which has a relatively small energy. These would be distributed uniformly over phase space, i.e. had we defined our cells as having constant length in  $\cos\theta$  all cells would receive essentially the same energy. We prefer to use  $\eta$  to parameterize the phase space, since the energy flow pattern will then be invariant under motion of the black hole along the beam pipe. Since  $d/d\eta = \sin^2(\theta)d/d\cos\theta$ , cells at small  $\cos\theta$ , i.e. small  $|\eta|$ , will then receive significantly more energy than those at large  $|\eta|$ . There should nevertheless be almost no empty cells; the maximal energy deposit, in cells with  $\eta \sim 0$ , would be about  $0.009E_{\text{tot}}$ , where  $E_{\text{tot}} \simeq 0.75M$  is the total hadronic energy released in the decay of a black hole with mass  $M$ . In particular, there should not be any cells with energy comparable to the initial average partonic energy, which amounts to about 300 GeV for our choices of parameters [see the discussion of Eq.(9) in Sec. 2]. The distribution expected for “ideal” chromospheres, with energy flow being completely independent of  $\phi$  and  $\cos\theta$ , is depicted by the blue step-like\* curves in Figs. 3.

In the opposite extreme, where the final state consists of a relatively small number [given by Eq.(9)] of very narrow jets, most cells would be empty, while in a few cells the deposited energy would be of order 300 GeV. However, even in the absence of parton-parton scattering, final state radiation implies that many jets will spread out over several cells. Together with the final hadronization step, this will lead to a significant number of cells in which a small, but nonzero, amount of energy is deposited, often in form of a single hadron. We therefore expect a non-trivial dependence on  $E_{\text{max}}$  in the entire range between  $\sim 100$  MeV and 1 TeV.

Our results for the energy flow of hadronic black hole decay products are shown in Figs. 3. We see that the number of cells with  $E < E_{\text{max}}$  indeed shows nontrivial dependence on  $E_{\text{max}}$  over a wide range. The number of (almost) empty cells decreases with increasing black hole mass, as expected from the higher initial parton multiplicity (9). However, even for  $M = 10$  TeV, in about 50% of the cells almost no energy is deposited; on the other hand, about twenty cells contain more than 100 GeV. We saw above that these results are consistent with the existence of well-defined jets. Parton-parton scattering has practically no effect on the number of cells containing at least 30 GeV, again indicating that it does not affect the jet structure at all.

---

\*These steps appear only for black hole decays at rest. In general one expects a smoothed-out version of these curves once a distribution of longitudinal momenta of the black holes is taken into account.

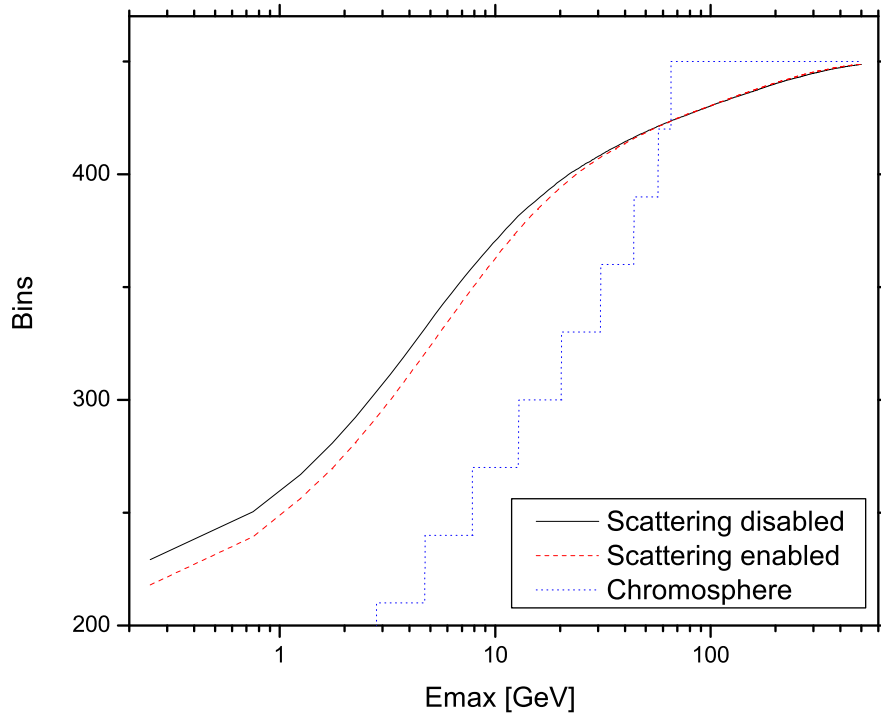
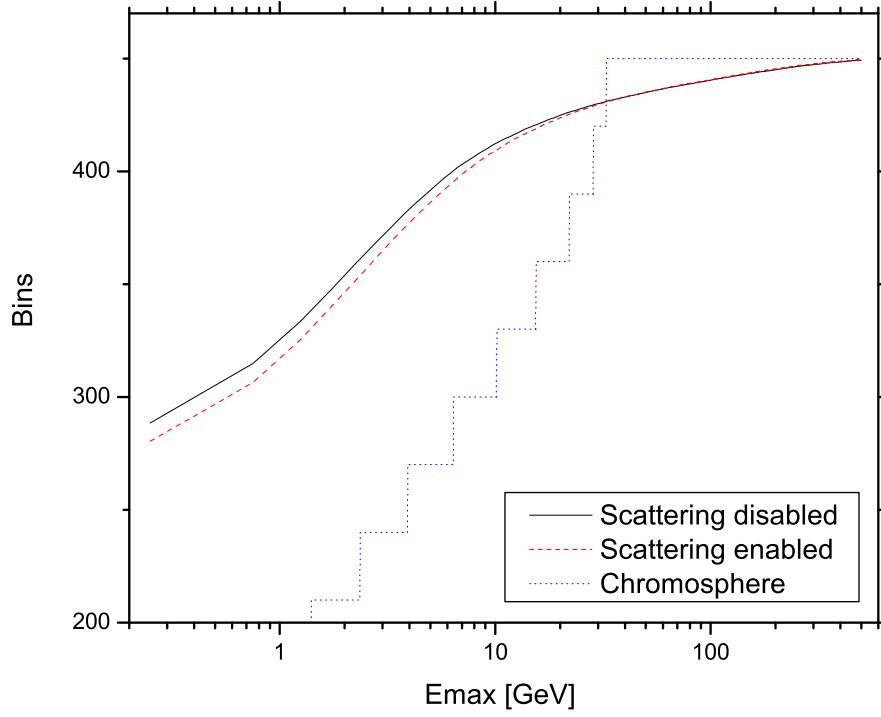


Figure 3: The number of phase space cells where the deposited energy satisfies  $E < E_{\max}$  as function of  $E_{\max}$ , for black hole mass  $M = 5$  TeV (top) and 10 TeV (bottom). The notation is as in Fig. 2, except that the blue, step-like, curves show the prediction from an ideal chromosphere.

Scattering does increase the total number of non-empty cells by about 5% (10%) for  $M = 5$  (10) TeV. However, the production of soft hadrons is a non-perturbative process, and can therefore not be treated from first principles; it is not clear whether the effect of parton-parton scattering is larger than the systematic error of our simulation.<sup>†</sup> Moreover, it should be kept in mind that the “underlying event”, which is created by the remnants of the colliding protons that do not participate in black hole formation, will also contribute a large number of (mostly soft) hadrons to the final state, which have not been included in our simulation. It is therefore not clear whether the increase of the cells containing some black hole decay products results in a measurable difference in the total energy flow in the event.

### 5.3 Microscopic structure of the events

The results of the two previous Subsections show that parton-parton interactions have little effect on the global characteristics of the hadronic final state that results from the decay of black holes with masses of a few TeV. In this Subsection we analyze the microscopic structure of the evolution of the hadronic final state that results from the decay of such black holes.

In Table 1 we list the average parton multiplicities (just before hadronization), as well as the average number of parton-parton collisions, for  $M = 5$  and 10 TeV. We see that even in the absence of parton-parton scattering, QCD branching (final state radiation) increases the multiplicity by an order of magnitude, relative to the initial multiplicity given by Eq.(9). We also see that the average number of parton-parton scatterings per black hole decay is not so small; as expected from simple statistical arguments, it increases roughly quadratically with the (initial or final) partonic multiplicity. Scattering increases the final parton multiplicity by 16% (23%) for  $M = 5$  (10) TeV. This effect is even larger than that on the number of non-empty calorimeter cells. Note, however, that the number of scatterings still remains well below the number of partons even for  $M = 10$  TeV.

| $M$ [TeV] | w/o scattering        |                       |                                     | with scattering       |                       |                                     |                                    |
|-----------|-----------------------|-----------------------|-------------------------------------|-----------------------|-----------------------|-------------------------------------|------------------------------------|
|           | $\langle n_q \rangle$ | $\langle n_g \rangle$ | $\langle n_{\text{parton}} \rangle$ | $\langle n_q \rangle$ | $\langle n_g \rangle$ | $\langle n_{\text{parton}} \rangle$ | $\langle n_{\text{scatt}} \rangle$ |
| 5         | 19                    | 116                   | 135                                 | 21                    | 134                   | 156                                 | 16                                 |
| 10        | 41                    | 241                   | 282                                 | 50                    | 295                   | 346                                 | 53                                 |

Table 1: Average final quark, gluon and total parton multiplicities from the decay of black holes with 5 and 10 TeV mass, with and without including the effect of parton-parton scattering. The last column gives the average number of partonic collisions. The statistical errors on the average multiplicities are about 2 percent.

---

<sup>†</sup>The *relative* size of the effect of parton scattering should be rather insensitive to the details of the simulation; the statement that it increases the number of non-empty cells by 5 to 10% should therefore be relatively robust. However, at the end one can only compare the *absolute* prediction of the simulation with actual events.

On the other hand, the probability  $\langle n_{\text{parton}} \rangle / \langle n_{\text{scatt}} \rangle$  that a given parton resulted from scattering is not negligible. It rises roughly linearly with the parton multiplicity, in agreement with the estimate (13). However, this expression, with  $Q_{\text{min}} \sim 1 \text{ GeV}$  as in our simulation, greatly over-estimates the number of scattering reactions even if we normalize it to the initial parton multiplicity.

As mentioned earlier, parton-parton scattering can only destroy the jet structure if it involves large momentum exchange, i.e. if the scale  $Q_{\text{scatt}}$  defined in Eq.(18) is large. In Fig. 4 we show a scatter plot of  $Q_{\text{scatt}}$  values vs. time in the simulation; here entries from 100 decays of black holes with mass  $M = 5 \text{ TeV}$  have been collected. We see that the average value of  $Q_{\text{scatt}}$  decreases with time, once  $t > 1/\langle E_{\text{parton}} \rangle \sim 3 \cdot 10^{-2} \text{ GeV}^{-1}$ . This can be understood from the observation that at early times, most partons are quite far off-shell; our condition (17) then implies that early scatterings must involve rather large momentum exchange. The existence of a few early scatterings with low  $Q_{\text{scatt}}$  is due to the fact that the initial virtualities with which the partons are actually created by the simulation may be much smaller than their maximal values, which is given by the energies of these partons.

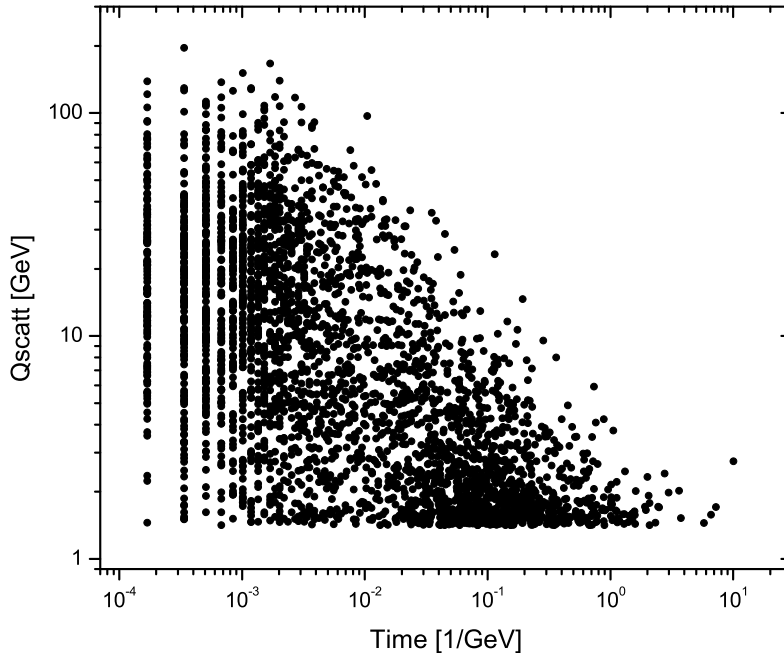


Figure 4: Scatter plot showing the scale  $Q_{\text{scale}}$  defined in Eq.(18) vs. time after black hole decay, for  $M = 10 \text{ TeV}$ ; scatterings from 100 decays have been added into this plot. The appearance of discrete lines at early times is an artefact of the finite time step size used.

Since the average virtualities of the partons diminish with increasing time, more scatterings with small  $Q_{\text{scatt}}$  become possible. Since the QCD cross sections satisfy  $d\sigma/dQ_{\text{scatt}}^2 \propto \alpha_s(Q_{\text{scatt}})^2 Q_{\text{scatt}}^{-4}$  if  $\hat{t}\hat{u} \ll \hat{s}^2$ , reactions with large  $Q_{\text{scatt}}$  are then greatly disfavored. Moreover, the average parton energies also decrease with time. Later collisions therefore tend to have smaller  $\hat{s}$ , which implies reduced kinematical upper bounds on  $Q_{\text{scatt}}$ .

The time dependence of the number of scattering reactions is determined by several competing effects. While the number of partons increases due to multiple branchings as time goes on, the number *density* of partons decreases, making it increasingly less likely that two partons will come close to each other. As a result, the number of collisions per unit time decreases at first. On the other hand, the decreasing virtuality of the partons, and corresponding decreasing lower bound on  $Q_{\text{scatt}}$ , means that their scattering cross section increases with time. This leads to an accumulation of relatively soft scatterings at  $t \sim 0.1/\text{GeV}$ .

A typical decay of a 5 TeV black hole therefore develops as follows. Initially there are about 12 highly off-shell partons with average energies around 300 GeV. One or two of them may undergo scattering very soon after their creation, with typical scattering scale  $Q_{\text{scatt}}$  of a few tens of GeV. Note that these rather hard reactions still mostly have  $Q_{\text{scatt}} \ll E$ , so that the direction of the participating partons is not changed very much. Moreover, these early scatterings may actually reduce the virtualities of the participating partons. As time goes on, the number of partons in the event increases, mostly due to branching processes. The number of scatterings also increases, but most of these reactions are relatively soft. We saw in Table 1 that they do increase the partonic multiplicity at the end of the QCD cascade. However, most of these scattering reactions involve partons inside the same jet, and therefore have little effect on the global quantities we analyzed in the previous Subsections. In fact, the creation of an additional very soft parton nearby in phase-space may not be visible in the (hadronic) final state at all. This explains why the results in Table 1 seem to indicate larger effects from parton-parton scattering than what we saw in Figs. 2 and 3.

## 6 Summary and conclusions

In this paper we investigated the question if the decays of black holes that might be produced at the LHC would be characterized by a relatively large number of discrete jets, as is usually assumed, or if they would lead to the formation of quasi-thermal “chromospheres” of rather soft hadrons, as suggested in ref.[15]. To this end we first described the partonic state produced by the decay of a black hole. We found that, if the higher-dimensional Planck mass  $M_D$  is at its current lower bound, the average initial number of partons will be less than about 25 for black holes with mass  $M \leq 10$  TeV, which might have a chance to be produced with appreciable rates at the LHC; higher values of  $M_D$  would lead to initial states with fewer partons, and hence to less scattering.

In Sec. 3 we summarized the argument in favor of formation of a chromosphere. We pointed out that this argument ignores the fact that scattering reactions take a finite

amount of time. Moreover, a very similar argument should apply to ordinary QCD multi-jet events. It would predict sizable effects in six jet events, which have been studied experimentally by the UA2 and CDF collaborations, who found good agreement with standard QCD predictions which ignore interactions between the partons in the final state.

Clearly a dedicated Monte Carlo study is required in order to determine the quantitative effects of such final state interactions on black hole events at the LHC. As described in Sec. 4, we wrote such a simulation code, based on the VNI program [32, 33]. We modified it by forcing scattering reactions to take a finite amount of time, which we estimated using the uncertainty principle. A very similar argument implies that, as time goes on, the parton system evolves towards smaller virtualities through branching processes. Scattering reactions may increase the virtualities of the participating partons again, but can also be a shortcut towards smaller virtualities.

Results of our simulation are described in Sec. 5. We found the effects of parton-parton scattering in the final state to be essentially negligible both for the angular correlation between energetic charged hadrons, and for the number of phase space cells containing a large amount of energy. We found some effect on the number of cells containing only one or a few soft hadrons. We interpreted these results in terms of the microscopic structure of the event. In particular, we saw that “hard” reactions, with large momentum exchange, only occur early on; in this case they may well reduce the virtualities of the participating partons. Later scatterings are all quite soft. At both early and late times, most scattering reactions have momentum exchange well below the energies of the participating partons; such reactions cannot significantly change the directions into which these partons are traveling. We therefore conclude that a chromosphere will *not* form; programs that ignore interactions between the partons from the decay of black holes created at the LHC only make a negligible mistake.

Our simulation has some shortcomings. Like all QCD simulation codes, it essentially works on the level of squared matrix elements, i.e. quantum mechanical interference effects can only be included in an approximate manner. In addition, we had to identify the quantum mechanical uncertainty in time with actual duration, both for the branching and scattering processes. It is not clear to us how this limitation can be overcome, even in principle.

Our results starkly contradict the claims of ref.[15], even though we chose our parameters and initial set-up such as to maximize the likelihood of scattering reactions between partons in the final state. It might therefore be worthwhile to summarize the three effects that have reduced the number of such reactions in our simulation.

Perhaps most important is that we only allow scattering of partons that approach each other. Interactions between partons that “always” (after their creation) move away from each other can certainly not be treated using the factorization into initial black hole decay and subsequent parton-parton scattering that underlies our simulation; for one thing, no  $S$ -matrix could be defined for such a state.\*

---

\*In some sense such partons can nevertheless still interact with each other. For example, the well-known Coulomb singularity [39] for near-threshold decays into charged particles can be interpreted in terms of the



Strictly speaking, in our case one cannot define an  $S$ -matrix for partons approaching each other, either, since they were created at a finite time, i.e. they did not exist in an “in-”state defined at time  $t = -\infty$ . We circumvent this problem by requiring the 4-momentum exchanged in these reactions to be larger than the initial virtualities. In this case one should be able to approximately treat the scattering like that of on-shell particles. This roughly means that we require scattering reactions to be fast on the time scale of the shower evolution up to the time of the scattering. This constraint greatly reduces the scattering cross section at early times, when the parton density is highest, and therefore reduces the number of scattering reactions. The fact that we do not allow partons participating in a scattering to start another scattering while the first one is still “in progress” has a much smaller effect on the number of these reactions.

Although the number of parton-parton collisions remains small for all black holes that might be produced at the LHC, we saw that it increases roughly quadratically with increasing black hole mass. Extrapolating from the results of Table 1, we estimate that there will be  $\mathcal{O}(1)$  parton-parton scatterings per produced parton once  $M \gtrsim 25$  TeV, if the higher-dimensional Planck scale  $M_D$  is kept at its lower bound of 0.65 TeV. This need not lead to formation of a chromosphere, however; we saw that most scattering reactions have little effect on the jet structure of the event. Note that in this case the average initial partonic multiplicity already exceeds 100, making the reconstruction of distinct jets quite unlikely, even if such heavy black holes could ever be produced at human-made colliders.

## Acknowledgments

The work of K.O. is partly supported by the Special Postdoctoral Researchers Program at RIKEN.

## References

- [1] N. Arkani-Hamed, S. Dimopoulos and G. R. Dvali, Phys. Lett. B **429** (1998) 263, hep-ph/9803315; I. Antoniadis, N. Arkani-Hamed, S. Dimopoulos and G.R. Dvali, Phys. Lett. B **436** (1998) 257, hep-ph/9804398.
- [2] L. Randall and R. Sundrum, Phys. Rev. Lett. **83** (1999) 3370, hep-ph/9905221.
- [3] G. 't Hooft, Phys. Lett. B **198** (1987) 61.
- [4] T. Banks and W. Fischler, hep-th/9906038.

---

electromagnetic interaction between these particles. However, in the simplest case of two-body decays, this singularity only affects the partial width for the decay; it does not increase the final state multiplicity. In case of decays into more than two partons, it can also change kinematical distributions, e.g. the invariant mass distributions of subsets of partons. However, a proper treatment of these effects would require the inclusion of corrections to black hole decays due to gauge loops. It is currently not clear how this could be done.

- [5] S. B. Giddings and S. D. Thomas, Phys. Rev. D **65** (2002) 056010, hep-ph/0106219.
- [6] S. Dimopoulos and G. Landsberg, Phys. Rev. Lett. **87** (2001) 161602, hep-ph/0106295.
- [7] D. M. Eardley and S. B. Giddings, Phys. Rev. D **66** (2002) 044011, gr-qc/0201034.
- [8] S. N. Solodukhin, Phys. Lett. B **533** (2002) 153, hep-ph/0201248.
- [9] S. D. H. Hsu, Phys. Lett. B **555** (2003) 92, hep-ph/0203154.
- [10] H. Yoshino and Y. Nambu, Phys. Rev. D **67** (2003) 024009, gr-qc/0209003.
- [11] H. Yoshino and V. S. Rychkov, Phys. Rev. D **71** (2005) 104028, hep-th/0503171.
- [12] R. C. Myers and M. J. Perry, Annals Phys. **172** (1986) 304.
- [13] S. W. Hawking, Commun. Math. Phys. **43** (1975) 199, [Erratum-ibid. **46** (1976) 206].
- [14] R. Emparan, G. T. Horowitz and R. C. Myers, Phys. Rev. Lett. **85** (2000) 499, hep-th/0003118.
- [15] L. Anchordoqui and H. Goldberg, Phys. Rev. D **67**, 064010 (2003), hep-ph/0209337.
- [16] C.M. Harris, P. Richardson and B.R. Webber, JHEP **0308** (2003) 033, hep-ph/0307305.
- [17] M. Cavaglia, R. Godang, L. Cremaldi and D. Summers, hep-ph/0609001.
- [18] S. Dimopoulos and R. Emparan, Phys. Lett. B **526** (2002) 393, hep-ph/0108060; K. Oda and N. Okada, Phys. Rev. **D66** (2002) 095005, hep-ph/0111298.
- [19] S. Hannestad and G.G. Raffelt, Phys. Rev. D **67** (2003) 125008 [Erratum-ibid. D **69** (2004) 029901], hep-ph/0304029.
- [20] Particle Data Group, W.-M. Yao et al., Journal of Physics G **33** (2006) 1.
- [21] L.A. Anchordoqui, J.L. Feng, H. Goldberg and A.D. Shapere, Phys. Rev. D **68** (2003) 104025, hep-ph/0307228.
- [22] L.A. Anchordoqui, J.L. Feng, H. Goldberg and A.D. Shapere, Phys. Lett. B **594** (2004) 363, hep-ph/0311365.
- [23] S. Hossenfelder, Phys. Lett. B **598** (2004) 92, hep-th/0404232.
- [24] D. Ida, K. Oda and S. C. Park, Phys. Rev. D **67** (2003) 064025, [Erratum-ibid. D **69** (2004) 049901], hep-th/0212108; and Phys. Rev. D **71** (2005) 124039, hep-th/0503052.

- [25] P. Kanti and J. March-Russell, Phys. Rev. D **66** (2002) 024023, hep-ph/0203223, and Phys. Rev. D **67** (2003) 104019, hep-ph/0212199; C.M. Harris and P. Kanti, JHEP **0310** (2003) 014, hep-ph/0309054, and Phys. Lett. B **633** (2006) 106, hep-th/0503010; G. Duffy, C. Harris, P. Kanti and E. Winstanley, JHEP **0509** (2005) 049, hep-th/0507274; M. Casals, P. Kanti and E. Winstanley, JHEP **0602** (2006) 051, hep-th/0511163; M. Casals, S.R. Dolan, P. Kanti and E. Winstanley, hep-th/0608193.
- [26] D. Ida, K. Oda and S. C. Park, Phys. Rev. D **73** (2006) 124022, hep-th/0602188.
- [27] V. Frolov and D. Stojkovic, Phys. Rev. D. **66** (2002) 084002, hep-th/0206046, and Phys. Rev. Lett. **89** (2002) 151302, hep-th/0208102; M. Cavaglia, Phys. Lett. B **569** (2003) 7, hep-ph/0305256; D. Stojkovic, Phys. Rev. Lett. **94** (2005) 011603, hep-ph/0409124.
- [28] A. Bonanno and M. Reuter, Phys. Rev. D **62** (2000) 043008, hep-th/0002196, and Phys. Rev. D **73** (2006) 083005, hep-th/0602159; S. Hossenfelder et al., Phys. Lett. B **575** (2003) 85, hep-th/0305262.
- [29] UA2 collab., J. Alitti et al., Phys. Lett. B **268** (1991) 145.
- [30] CDF collab., F. Abe et al., Phys. Rev. D **56** (1997) 2532.
- [31] G. Marchesini and B.R. Webber, Nucl. Phys. B **238** (1984) 1.
- [32] K. Geiger, R. Longacre and D. K. Srivastava, nucl-th/9806102.
- [33] S. A. Bass, M. Hofmann, M. Bleicher, L. Bravina, E. Zabrodin, H. Stoecker and W. Greiner, Phys. Rev. C **60** (1999) 021901, nucl-th/9902055. The code is available from <http://www.phy.duke.edu/~bass/vni.html> .
- [34] T. Sjöstrand, L. Lonnblad, S. Mrenna and P. Skands, hep-ph/0308153.
- [35] See <http://www.gnu.org/software/gsl>.
- [36] K. Geiger and B. Müller, Nucl. Phys. B **369** (1992) 600.
- [37] M. Bengtsson and T. Sjöstrand, Nucl. Phys. B **289** (187) 810.
- [38] B. R. Webber, Ann. Rev. Nucl. Part. Sci. **36** (1986) 253.
- [39] See e.g. J. Schwinger, “Particles, Sources and Fields”, Vol. II (Addison–Wesley, Reading, MA, 1970/73).

